Desalination and Water Treatment
www.deswater.com
doi: 10.5004/dwt.2020.26085

201 (2020) 195–203
October

Behavior of anthocyanins in the presence of cassava starch (a biocomposite with antioxidants properties)

J.J. García-Sánchez[a], M. Solache-Ríos[b], R. Sánchez-Orozco[a], M.C. Díaz-Nava[c,*]

[a]*Tecnológico de Estudios Superiores de Jocotitlán, Carretera Toluca-Atlacomulco Km 44.8, Ejido San Juan y San Agustín, C.P. 50700 Jocotitlán, Estado de México, México, emails: jjuangs1@gmail.com (J.J. García-Sánchez), rsanchez_o@yahoo.com.mx (R. Sánchez-Orozco)*
[b]*Instituto Nacional de Investigaciones Nucleares, Depto. de Química. Apdo. Postal 18-1027, C.P. 11801 Ciudad de México, México, email: marcos.solache@inin.gob.mx (M. Solache-Ríos)*
[c]*Instituto Tecnológico de Toluca, Av. Tecnológico s/n. Colonia Agrícola Bellavista, Metepec, Edo. De México, México C.P. 52149, email: cardinava.posgrado@gmail.com (M.C. Díaz-Nava)*

Received 20 January 2020; Accepted 10 May 2020

ABSTRACT

The adsorption of the calyx extract of *Hibiscus sabdariffa L.* (a natural pigment) onto cassava starch (CS) was evaluated in order to develop a simple and efficient process of separation and to obtain a biocomposite with antioxidant properties. The diffusion mechanism of anthocyanin on the adsorbent was analyzed, considering pH, contact time and adsorbent dosage. Dye adsorption equilibrium was reached after 12 h of contact time, and it was described by the pseudo-second-order kinetic and intra-particle diffusion models. Adsorption equilibrium data were treated with Langmuir, Temkin and Freundlich adsorption isotherms models over the entire adsorbent dosage from 0.1 to 2.0 g. The adsorbent used was characterized by surface acidity, point of zero charge, Fourier-transform infrared spectroscopy and scanning electron microscopy before and after the adsorption of anthocyanins. The content of anthocyanins in the cassava starch was 1.3 ± 04 mg g^{-1}. This study is useful to evaluate the industrial production of a biocomposite rich in antioxidants and the potential application of anthocyanin as a pigment in the food.

Keywords: Adsorption; Anthocyanins; Cassava starch; *Hibiscus sabdariffa L.*

1. Introduction

The food and cosmetic industries use many toxic synthetic dyes and in recent years there is a growing interest in natural dyes because they are less toxic, non-carcinogenic, non-poisonous and environment friendly. The natural dyes are obtained from plants, animals and minerals, and have different colors like red, yellow, blue, black, brown and a combination of them [1–4]. Some plants can be used as additives due to their color and antioxidant properties. *Hibiscus sabdariffa L.* (Roselle) is a natural dye source, the calyces have an intense red color and are a source of natural anthocyanins. The anthocyanins are some of the most used natural food additives due to their antioxidant action and intense color.

The extraction of anthocyanins can be tedious with a high cost, low efficiency and longtime extraction. Technical knowledge helps to reduce costs and improve efficiency so that research has been conducted for anthocyanins purification by different processes like using high carbon dioxide pressure and water as solvent [5]; liquid chromatography using water/ethanol/formic acid mixture circulating in a closed-loop system [6] and an aqueous two-phase

* Corresponding author.

system [7]. Anthocyanin was obtained with high purity by these processes, however, the extraction using CO_2 requires high pressures, produces a high percentage of waste and it is not viable at the pilot-scale because of the complexity of the system.

The adsorption may be a viable alternative because it is environmentally friendly and cost-effective. Previous studies have used different adsorbents for the separation of anthocyanins from liquid extracts: mesoporous silica containing small amounts of aluminum and iron, synthetic layered silicate, chitosan films, macroporous resins, amberlite, activated charcoal, and bentonite [8–12].

Starch is a biopolymer and is present in living plants as energy storage material. Most starches contain only a single type of carbohydrate (glucose) and form two polymer chains, a linear chain molecule (amylose) and a branched polymer of glucose (amylopectin) [13]. The high level of amylopectin on starch may help with the adsorption of anthocyanins. Starch can be obtained from the roots of the cassava plant. Cassava starch is different from other starches due to its low level of residual materials, its amylose content is lower than other amylose-containing starches, and contains high molecular weights of amylose and amylopectin. The food industry generally uses tapioca starch as a thickener and stabilizer. The non-contribution of flavor in food systems, starches allow the complete and immediate retention of the flavor of the food itself.

The aim of this work was to extract anthocyanin pigments from the calyx extract of *Hibiscus sabdariffa L.* in aqueous solution and its separation by adsorption onto cassava starch. The determination of the physicochemical interactions can be used to evaluate the industrial production of a biocomposite rich in antioxidants and the possible application of anthocyanin as a pigment in the food.

2. Materials and methods

2.1. Materials

Tapioca pearls were used as cassava starch (*Manihot esculenta Crantz*), pearls, and hibiscus flowers (*Hibiscus sabdariffa L.*) were obtained from the local market.

2.2. Extract of hibiscus flowers

The hibiscus flowers were oven-dried and pulverized. The hibiscus flower extract (HFE) was obtained as follows: 1 g of hibiscus flower powder and 100 mL of distilled water was heated at 60°C for 1 h. The mixture was filtered, cooled at room temperature and kept at 4°C in dark until further use.

2.3. Characterization

2.3.1. Point of zero charge (PZC)

The point of zero charge of the cassava starch (CS) was determined by the following process [14,15]: 50 mL aliquots of a 0.1 M sodium chloride solution were placed in different flasks and their pH was adjusted to values within 4–10 range through the addition of 0.1 M HCl or NaOH solutions, then 1 g of cassava starch was added to each flask and the mixtures were left for 24 h with continuous stirring at 100 rpm. Finally, the pH was measured and pH_{PZC} was graphically determined as the point at which the pH variation against initial pH crosses the line at which its value is zero.

2.3.2. Acidity and basicity of the surface

Both the surface acidity and basicity of CS were determined by a titration method reported by Moreno-Castilla et al. [16]. CS was washed several times with distilled water and then dried at 100°C for 24 h.

Acidity or basicity of CS surface was determined as follows: 1 g of the adsorbent and 50 mL of 0.1 N of NaOH or HCl solutions were shaken at 30°C for 5 d using an automatic shaker. The mixtures were filtered and then back-titrated with a 0.1 N HCl or NaOH solution. The concentrations of acidic and basic groups on the surface were calculated and expressed as eq g^{-1}.

2.3.3. Scanning electron microscopy

In order to investigate the morphology of the material, the samples were mounted directly on the holders and then observed at 10 and 20 kV in a JEOL JSM-5900-LD electron microscope. The elemental analysis was done with an energy X-ray dispersive spectroscopy (EDS) system.

2.3.4. Fourier-transform infrared spectroscopy

IR spectroscopy was used to determine the functional groups responsible for HFE sorption, about 0.1 g of biomass was mixed with KBr for Fourier-transform infrared spectroscopy analysis with a resolution of 2 cm^{-1}.

2.4. Adsorption of HFE on cassava starch

The adsorption assays were performed in a batch system, cassava starch (1.0 g of dry starch) and 10 mL HFE (pH 2.5) were mixed at room temperature and shaken at 80 rpm for 24 h, then the mixture was filtered. The amount of HFE in the remaining solution was determined by ultraviolet-visible (UV-Vis) spectrophotometry analysis at 664.5 nm. The sorption percent was calculated as follows [17]:

$$\text{Color sorption}(\%) = \frac{\text{Initial absorbance} - \text{Observed absorbance}}{\text{Initial absorbance}} \times 100 \quad (1)$$

The adsorption at time t, q_t (mg g^{-1}), was calculated by using the following equation:

$$q_t = \frac{(C_0 - C_t)V}{(W)} \quad (2)$$

where C_t (mg L^{-1}) is the liquid-phase concentrations of HFE at time t, C_0 (mg L^{-1}) is the initial concentration of the HFE in solution. V is the volume of the solution (L) and W is the mass of cassava starch (g).

The quantities of adsorbents used to determine the effect of sorbent dose were 10, 20, 40, 60, 80, 100, 120, 140, 160, 180, and 200 mg. The contact times considered for the adsorption

kinetics were 0.08, 0.25, 0.5, 1, 3, 5, 7, 24, 48, and 72 h, and the effect of pH on the adsorption of anthocyanin pigments was determined from initial pH from 2 to 12.

The equilibrium data were fitted to three different adsorption isotherms models; Freundlich [18,19], Langmuir [20,21] and Temkin [22,23]. The kinetics data were fitted to pseudo-first-order [24,25], pseudo-second-order [26,27], intra-particle diffusion [28,29], and Elovich [30] models (Table 1).

2.5. Adsorption and desorption of anthocyanins

1 g of cassava starch and 20 mL of HFE were mixed in a 50 mL flask. The mixture was shaken at room temperature at 80 rpm for 24 h. After adsorption, the mixture was filtered and the anthocyanin was determined in the aqueous solution. For desorption, 1 g of anthocyanins saturated cassava starch was mixed with 20 mL of water and left for 24 h at room temperature, then the cassava starch was separated from the remaining aqueous solution and the anthocyanin was measured in this solution. Adsorption/desorption ratio and capacities were calculated using the following equations [31]:

$$\text{Adsorption capacity}, q_e\left(\text{mg/g}\right) = C_0 - C_e \times \frac{V_i}{\left(1-M\right)W} \tag{3}$$

$$\text{Desorption capacity}, q_d\left(\text{mg/g}\right) = \frac{C_d V_d}{\left(1-M\right)W} \tag{4}$$

where q_e is the adsorption capacity (mg g^{-1}) at equilibrium, C_0 (mg L^{-1}) is the initial anthocyanin concentration in the extract, and C_e (mg L^{-1}) is the equilibrium anthocyanin concentration in the extract. V_i (mL) is the volume of the crude extract; W (g) is the mass of the starch, and M is the moisture content of the starch (wt%/wt%). C_d (mg L^{-1}) and V_d are the concentration of anthocyanin and the volume of the remaining solution (mL) after the desorption process respectively.

2.6. Determination of anthocyanin content

The pH differential method can be used to determine the total monomeric anthocyanin content, based on the structural change of the anthocyanin chromophore between pH 1.0 and 4.5 [32]. This method permits an accurate and rapid measurement of the total anthocyanins, even in the presence of degraded polymerized pigments and other interfering compounds. Anthocyanin pigment concentration (expressed as cyanidin-3-glucoside equivalents) was calculated as follows:

$$\text{Anthocyanin pigment}\left(\text{cyanidin-3-glucoside equivalents,mg/L}\right) = \frac{A \times \text{MW} \times \text{DF} \times 10^3}{\varepsilon \times l} \tag{5}$$

where A is the absorbance of each dilution; MW (molecular weight) = 449.2 g mol^{-1} for cyanidin-3-glucoside (cyd-3-glu); DF = dilution factor; l = pathlength in cm; ε = 26,900 molar extinction coefficient, in L × mol^{-1} × cm^{-1}, for cyd-3-glu; and 10^3 = factor for conversion from g to mg.

The absorbance of the diluted sample (A) was calculated as follows:

$$A = \left(A_{\lambda\text{vis}-\max} - A_{700}\right)\text{pH1} - \left(A_{\lambda\text{vis}-\max} - A_{700}\right)\text{pH 4.5} \tag{6}$$

The dilution was done with potassium chloride buffer for pH 1.0, and with sodium acetate buffer for pH 4.5.

2.6. Statistical analysis

All experiments were performed at least twice, and the results were expressed considering the standard deviations. The data were fitted to models with the help of Microsoft Excel.

3. Results and discussion

3.1. Physicochemical properties of adsorbent and solute

Table 2 shows a summary of the physicochemical properties of the surface of the cassava starch. The moisture percentage of the cassava starch was 13.4%. The surface of cassava starch possesses an evident basic character and a pH_{pzc} value of 6.0 (Fig. 1). The basic character suggests that cassava starch is an efficient material to remove anionic species (acid dyes).

Total soluble solids (TSS) in a solution is determined by the index of refraction. It is measured using a refractometer, it is referred to as the degrees Brix and it is equivalent to TSS content (%). The sample (HFE) contains 15°Brix which is equivalent to a TSS content of 15%.

The total acidity and pH are different: the pH is the property most useful in extract biochemistry. The total acidity of the HFE is an important property, because influences the taste, freshness and protection from spoiling micro-organisms; a low acidity level is much more susceptible to organisms. The color of anthocyanins depends on the pH of the solution because of the molecular structure of anthocyanins has an ionic nature [33]. It is important to note that the extract showed similar spectra at pH values ≤5, which indicates that it is stable in this pH range. The HFE in acidic condition appears to be red, in neutral pH has a purple hue while the color changes to blue in basic pH.

3.2. Characterization of HFE-CS powder

3.2.1. Microstructure and elemental composition

The scanning electron microscopy images of cassava starch show a granular aspect, with particles of different shapes and sizes (Fig. 2a). The cassava starch particles show porous of irregular sizes and agglomerations of small particles on the surfaces (Fig. 2b). Probably, the adsorption of dye takes place inside the pore of starch (intra-particle diffusion), some surface fissures are observed on the starch granule that could allow the solute to get into them.

The elemental compositions of both native and modified starches were determined by EDS. The presence of carbon and oxygen were found in both starches. The presence of some elements (Mg, Si, Cl, K, Ca) in the modified starch is evidence of the adsorption of the HFE by the starch (Table 3).

Table 1
Mathematical models used for the analyses of the moisture and hibiscus flowers extract adsorption by cassava starch

Model	Non-linear equation	Linear equation	
Kinetics			
Pseudo-first-order	$q_t = q_e\left(1-e^{-Kt}\right)$	$\ln\left(q_e - q_t\right) = \ln q_e - K_1 t$	(7)
	where q_e is the amount of dye adsorbed onto the adsorbent at equilibrium (mg g^{-1}), q_t is the amount of dye adsorbed onto the adsorbent at any time t (mg g^{-1}), and K_1 (min^{-1}) is the rate constant of the pseudo-first-order adsorption.		
Pseudo-second-order	$q_t = \frac{K_2 q_e^2 t}{1+K_2 q_e t}$	$\frac{t}{q_t} = \frac{1}{K_2 q_e^2} + \frac{1}{q_e} t$	(8)
	where K_2 (g mg^{-1} min^{-1}) is the rate constant of the pseudo-second-order adsorption, q_e is the amount of dye adsorbed on the adsorbent at equilibrium (mg g^{-1}), and q_t is the amount of dye adsorbed on the adsorbent at any time, t (mg g^{-1}).		
Intra-particle diffusion equation	$q_t = K_{\text{ipd}} t^{1/2} + C_i$	$\log q_t = \log K_{\text{ipd}} + 0.5 \log t$	(9)
	where q_t is the amount of dye adsorbed onto the adsorbent at time t (mg g^{-1}), C_i is the intercept, and K_{ipd} is the intra-particle diffusion rate constant (mg g^{-1} min$^{-0.5}$).		
Elovich	$\frac{dq_t}{d_t} = \alpha \exp\left(-\beta q_t\right)$	$q_t = \frac{1}{\beta}\ln\left(\alpha\beta\right) + \frac{1}{\beta}\ln\left(t\right)$	(10)
	where q_t is the amount of dye sorbed by CS at a time t, α is the initial dye sorption rate (mg g^{-1} min^{-1}) and β is the desorption constant (g mg^{-1}) during any one experiment.		
Isotherm			
Langmuir	$q_e = \frac{q_m b_L C_e}{1+b_L C_e}$	$\frac{1}{q_e} = \frac{1}{q_m} + \frac{1}{q_m K_L C_e}$	(11)
	where q_e is the amount of dye adsorbed (mg g^{-1}), C_e is the equilibrium concentration of the adsorbate (mg L^{-1}), and q_m and K_L are Langmuir constants related to the maximum adsorption capacity (mg g^{-1}) and energy of adsorption (L mg^{-1}).		
Freundlich	$q_e = K_F C_e^{1/n}$	$\log q_e = \log K_F + \frac{1}{n}\log C_e$	(12)
	where q_e is the amount adsorbed at equilibrium (mg g^{-1}), K_F is the Freundlich constant, $1/n$ is the heterogeneity factor which is related to the capacity and intensity of the adsorption, and C_e is the equilibrium concentration (mg L^{-1}).		
Temkin	$q_e = \frac{RT}{b_T}\ln\left(K_T C_e\right)$	$q_e = B \ln K_T + B \ln C_e$ $B = \frac{RT}{b_T}$	(13)
	where K_T is the Temkin isotherm equilibrium binding constant (L g^{-1}), b_T is the Temkin isotherm constant, R is the universal gas constant (8.314 J mol^{-1} K^{-1}), T is the Temperature at 298 °K, B is the constant related to heat of sorption (J mol^{-1}).		

3.2.2. Infrared spectroscopy

Several characteristic bands of starch and water were observed in the spectra of cassava starch (Fig. 3a). An intense band in the range of 3,600–3,200 cm^{-1} is generated by stretching vibration of O–H bond. Bands in the range of 3,000–2,800 cm^{-1} are assigned to stretching vibrations of the C–H bond. The peak found at 1,300 cm^{-1} belongs to the symmetric stretching of –CH_2. The wide absorption bands in the range of 1,000–1,200 cm^{-1} are characteristic of the C–O stretching, C–O–C structure and C–O–H of the glycosidic ring of the starch. Bands in the range of 1,700–1,600 cm^{-1} were observed in the modified starch spectra and probably are due to tightly bound water to the starch molecules (Fig. 3b).

3.3. Isotherm and kinetics on the retention of dye (HFE) by cassava starch

Adsorption studies were done considering concentration, time, and pH. The adsorption efficiency of cassava

Table 2
Properties of the cassava starch (CS) and extract of hibiscus flowers extract (HFE)

Properties of the surface of CS	
Moisture content	13.4%
Basic character	2.5 eq g^{-1}
Acid character	0.42 eq g^{-1}
pH_{pzc}	6.0
aW	0.6
Properties of HFE	
Brix	15
pH	2.4
Acidity (%)	0.11

Table 3
Elemental composition

Element (%)	CS	E-CS
C	54.70	48.94
O	46.30	48.17
Mg		0.18
Si		0.37
Cl		0.20
K		1.60
Ca		0.55
Total	100.00	100.00

CS, cassava starch;
E-CS, cassava starch treated with extract of hibiscus flowers.

starch was 63.2% at the equilibrium time of 12 h with an HFE initial concentration of 0.5 g mL^{-1}. In general, the red color of HFE was removed optimally in the pH range from 2 to 4 (Fig. 4). This behavior can be explained by the zero-point charge of the adsorbent (pH_{ZPC} = 6.0), at a pH above this

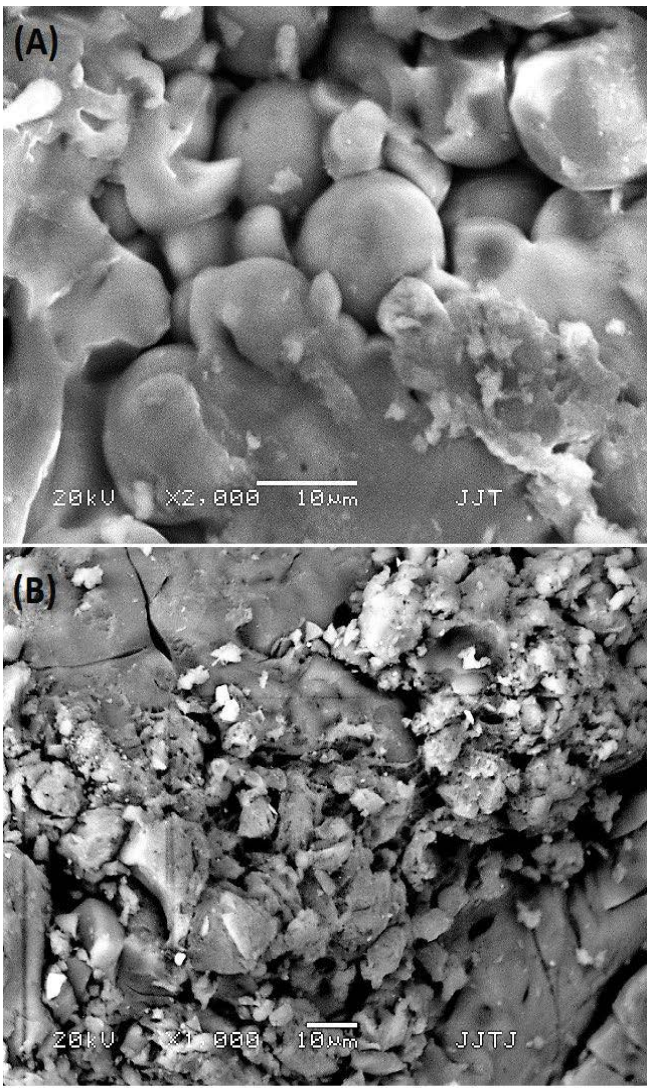

Fig. 2. Micrograph of cassava starch sample by scanning electron microscopy (SEM).

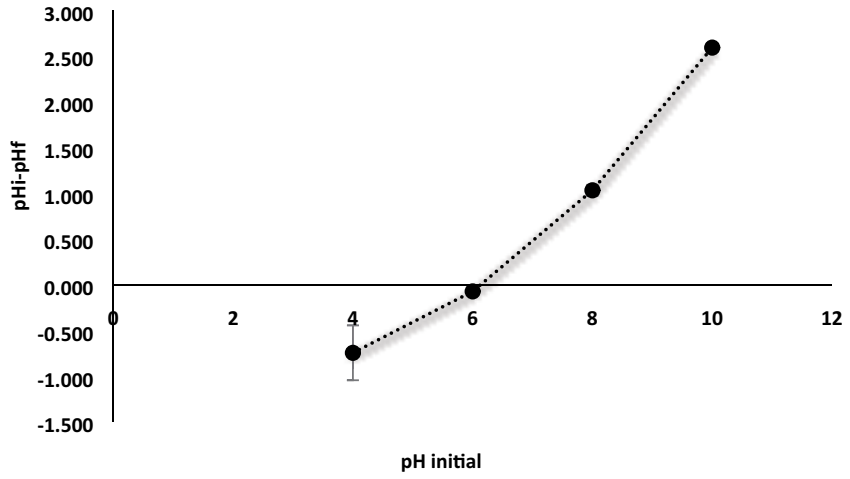

Fig. 1. The pH_{PZC} of cassava starch.

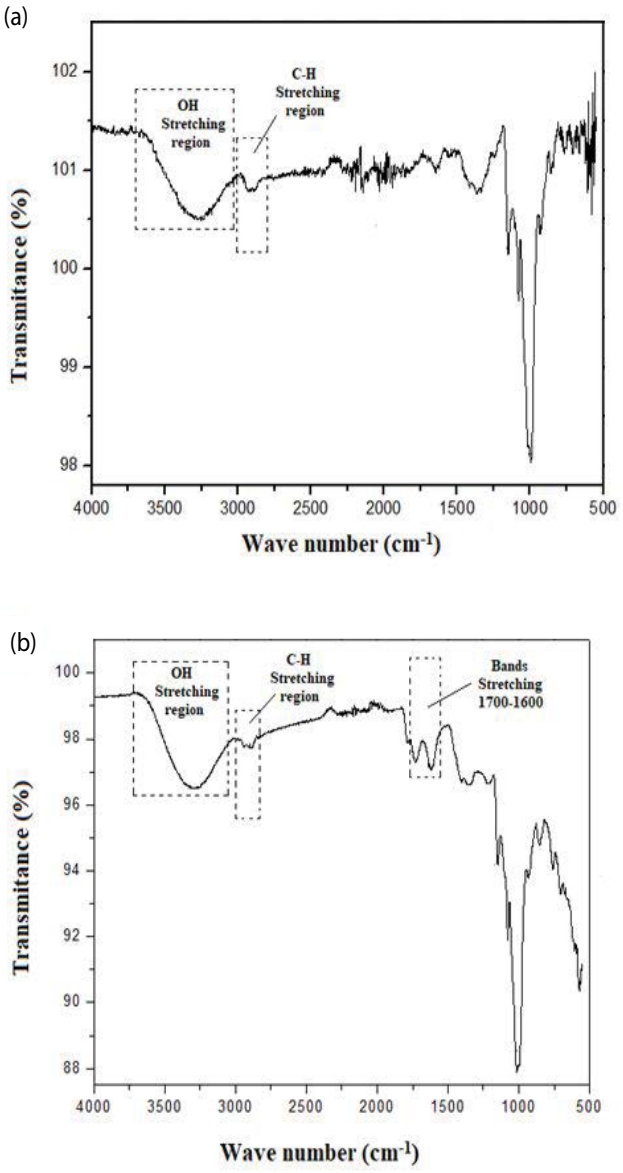

Fig. 3. Fourier-transform infrared spectroscopy of the native and modified starch.

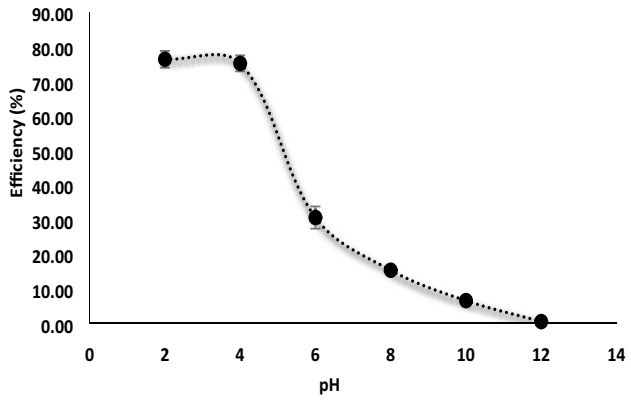

Fig. 4. Effect of pH on adsorption capacity

zero-point charge, the surface of the adsorbent is negative, which does not enhance the adsorption.

The adsorption kinetics of anthocyanin pigments onto starch was evaluated using pseudo-first-order, pseudo-second-order, Elovich and intra-particle diffusion models, however, the pseudo-first-order model did not fit with the experimental data well. The correlation coefficient for the second-order kinetic model obtained was the highest for this model (Fig. 5) with a value for the adsorption rate constant of 0.088 g mg^{-1} min^{-1}. The adsorption capacity in the equilibrium (35.6 mg g^{-1}) is similar to the one calculated from the second-order kinetic model (Table 4). This behavior

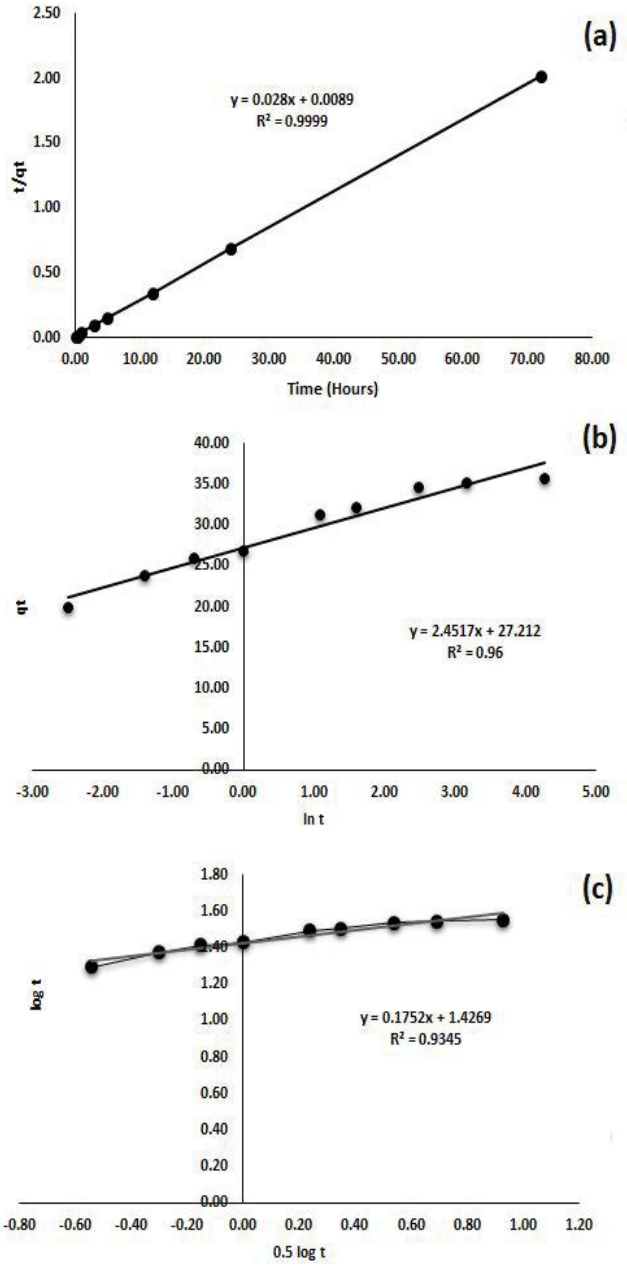

Fig. 5. Kinetic models of dye adsorption on starch (a) pseudo-second-order, (b) Elovich, and (c) intraparticle diffusion.

Table 4
Parameters from the fitting of experimental data to kinetics and isotherm models

Kinetics parameters for the adsorption of color						
Pseudo-second-order				Elovich		
K_2 (g mg^{-1} min^{-1})	q_e (mg g^{-1})	R^2		α (mg g^{-1} min^{-1})	β (g mg^{-1})	R^2
0.088	35.7	0.9999		162,755	0.41	0.96
Intra-particle diffusion						
K_{ipd} (mg g^{-1} min$^{-0.5}$)	C_i	R^2				
0.175	1.426	0.9309				
Isotherm parameters for the adsorption of color						
Freundlich				Temkin		
n	K_F (L g^{-1})	$1/n$	R^2	K_T (L g^{-1})	B (J mol^{-1})	R^2
0.68	1.7×10^{-3}	1.48	0.9468	2.4×10^{-3}	57.38	0.8848

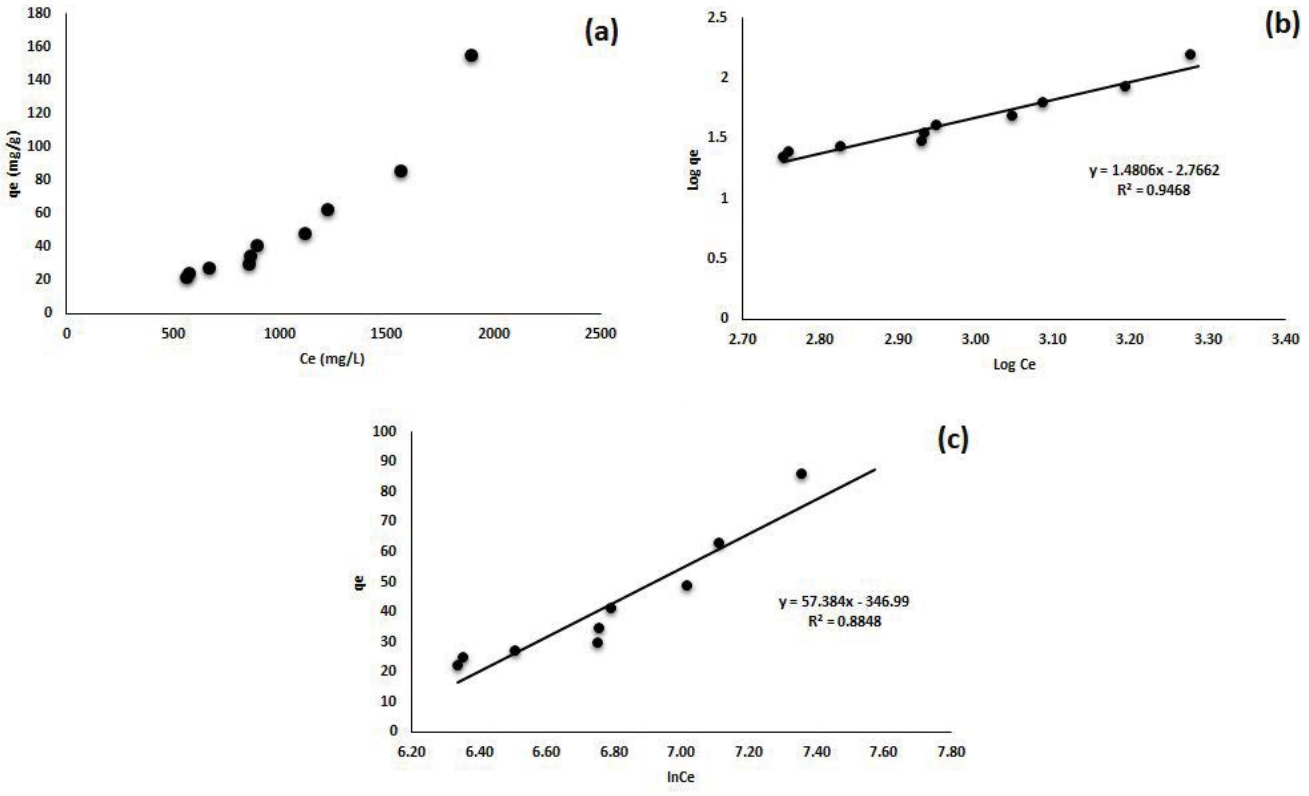

Fig. 6. Different isotherm models (a) experimental adsorption isotherm, (b) Freundlich adsorption isotherm, and (c) Temkin adsorption isotherm.

indicates that the adsorption mechanism is chemisorption which involves valence forces through sharing or exchange of electrons between the sorbent and the sorbate. The small value of the intra-particle diffusion constant indicates that the boundary layer has a low effect on the diffusion mechanism of HFE uptake by the cassava starch.

Similar behavior was observed in the adsorption of *Hibiscus sabdariffa* sp. anthocyanins onto a macroporous resin, the adsorption kinetic experimental data fitted the pseudo-second-order kinetic model [11,34].

The adsorption isotherm describes the retention behavior of the HFE on the cassava starch at constant pH and temperature. The adsorption isotherm has a Freundlich or linear shape (Fig. 6), the isotherm data of HFE were adjusted to Freundlich and Temkin isotherm model and the parameters obtained are shown in Table 4. The R^2 value for the Freundlich

model was higher than the Temkin isotherm model, these results indicate that the adsorption takes place on a surface with heterogeneous distribution of active sites and the adsorption depends on the concentration of the solute.

The adsorption isotherm of *Hibiscus sabdariffa* sp. anthocyanins onto a macroporous resin was Langmuir isotherm type [11,34], this behavior could be due to the nature of the adsorbent.

3.4. Total monomeric anthocyanin retained on the starch

The proposed method (pH – differentia) was applied to determine the anthocyanin content. The anthocyanin concentration present in the extract was 4.06 mg L^{-1}, the average adsorption capacity and desorption of anthocyanin were 1.3 ± 0.4 mg g^{-1} and 0.07 ± 0.01 mg g^{-1} respectively. Similar phenomena were observed in the adsorption and desorption of anthocyanin in an aqueous solution of purple rice bran using amberlite XAD7, where the values were 1.87 and 1.79 mg g^{-1}, respectively [12].

The retention capacity of anthocyanins on cassava starch was evaluated with different amounts (0.5, 1.0, 1.5, 2.0 and 2.5 g) of starch and 20 mL of the solution of HFE (1 g/100 mL), as shown in Fig. 7. As can be observed there is a linear correlation between adsorption of anthocyanins and CS dosage with a correlation coefficient of 0.9698, the adsorption of anthocyanins increases as the quantity of CS increases.

4. Conclusions

The present study provides insights on diffusion and adsorption of anthocyanin from HFE by cassava starch. The following conclusions can be drawn: The anthocyanin molecule's immobilization on cassava starch was favored in the interaction solid-liquid system with a maximum color removal efficiency of 63.2% at room temperature and 1 g of CS. The red dye was removed optimally in acid pH. The experimental adsorption data best fit Freundlich and pseudo-second-order kinetic models. It is suggested that the adsorption of dye was inside the pore of starch (intra-particle diffusion). The amount of dye adsorbed on the starch was 36.6 mg g^{-1} with the content of Roselle anthocyanins of 1.3 mg g^{-1}.

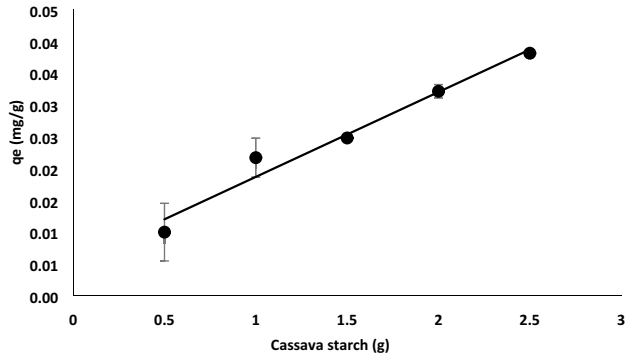

Fig. 7. Effect of dosage on the adsorption of anthocyanin by cassava starch.

The appreciable amount of anthocyanin compounds adsorbed on starch provides a significant antioxidant capacity that may be of great interest for health with applications in the food industry.

References

[1] A. Manikandan, M. Durka, M.A. Selvi, S.A. Antony, Sesamum indicum plant extracted microwave combustion synthesis and opto-magnetic properties of spinel $Mn_xCo_{1-x}Al_2O_4$ nano-catalysts, J. Nanosci. Nanotechnol., 16 (2015) 448–456.
[2] A. Manikandan, M. Durka, M.A. Selvi, S.A. Antony, Aloe vera plant extracted green synthesis, structural and opto-magnetic characterizations of spinel Co(*x*) $Zn_{1-x}Al_2O_4$ nano-catalysts, J. Nanosci. Nanotechnol., 16 (2016) 357–373.
[3] P. Bhavani, A. Manikandan, P. Paulraj, A. Dinesh, M. Durka, S.A. Antony, Okra (*Abelmoschus esculentus*) plant extract-assisted combustion synthesis and characterization studies of spinel $ZnAl_2O_4$ nano-catalysts, J. Nanosci. Nanotechnol., 18 (2018) 4072–4081.
[4] N. Babitha; L.S. Priya, S.R. Christy, A. Manikandan, A. Dinesh, M. Durka, S. Arunadevi, Enhanced antibacterial activity and photo-catalytic properties of ZnO nanoparticles: pedalium murex plant extract-assisted synthesis, J. Nanosci. Nanotechnol., 19 (2019) 2888–2894.
[5] G. Jiao, A. Kermanshahi pour, Extraction of anthocyanins from haskap berry pulp using supercritical carbon dioxide: influence of co-solvent composition and pretreatment, LWT Food Sci. Technol., 98 (2018) 237–244.
[6] C.G. Grigoras, E. Destandau, S. Zubrzycki, C. Elfakir, Sweet cherries anthocyanins: an environmental friendly extraction and purification method, Sep. Purif. Technol., 100 (2012) 51–58.
[7] A.S. Lima, C.M.F. Soares, R. Paltram, H. Halbwirth, K. Bica, Extraction and consecutive purification of anthocyanins from grape pomace using ionic liquid solutions, Fluid Phase Equilib., 451 (2017) 68–78.
[8] Y. Kohno, Y. Kato, M. Shibata, C. Fukuhara, Y. Maeda, Y. Tomita, K. Kobayashi, Enhanced stability of natural anthocyanin incorporated in Fe-containing mesoporous silica, Microporous Mesoporous Mater., 203 (2015) 232–237.
[9] C. Capello, G.L. Coelho, C.E.M. Campos, D. Hotza, B.A.M. Carciofi, G.A. Valencia, Adsorption and desorption of eggplant peel anthocyanins on a synthetic layered silicate, J. Food Eng., 262 (2019) 162–169.
[10] V.L. Carvalho, J.O. Goncalves, A. Silva, T.R. Cadaval Jr., L.A.A. Pinto, T.J. Lopes, Separation of anthocyanins extracted from red cabbage by adsorption onto chitosan films, Int. J. Biol. Macromol., 131 (2019) 905–911.
[11] C. Xiu-Lian, D. Wang, C. Bi-Yun, F. Yong-Mei, W. Shao-Hong, Z. Peng-Yuan, Adsorption and desorption properties of macroporous resins for anthocyanins from the calyx extract of roselle (*Hibiscus sabdariffa L.*), J. Agric. Food. Chem., 60 (2012) 2368−2376.
[12] A. Baran Das, V.V. Goud, C. Das, Adsorption/desorption, diffusion, and thermodynamic properties of anthocyanin from purple rice bran extract on various adsorbents, J. Food Process Eng., 41 (2018) e12834. https://doi.org/10.1111/jfpe.12834
[13] E. Bertoft, Analyzing Starch Structure, A.C. Eliasson, Ed., Starch in Food. Structure, Function and Applications, CRC Press, New York, 2004, pp. 57–96.
[14] B.M. Babić, S.K. Milonjić, M.J. Polovina, B.V. Kaludierović, Point of zero charge and intrinsic equilibrium constants of activated carbon cloth, Carbon, 37 (1999) 477–481.
[15] J.W. Shim, S.J. Park, S.K. Ryu, Effect of modification with HNO_3 and NaOH on metal adsorption by pitch-based activated carbon fibers, Carbon, 39 (2001) 1635–1642.
[16] C. Moreno-Castilla, E. Carrasco-Marín, E. Utrera-Hidalgo, J. Rivera-Utrilla, Activated carbons as adsorbents of SO_2 in flowing air. Effect of their pore texture and surface basicity, Langmuir, 9 (1993) 1378–1383.

[17] T. Teka, S. Enyew, Study on effect of different parameters on adsorption efficiency of low cost activated orange peels for the removal of methylene blue dye, Int. J. Innovation Sci. Res., 8 (2014) 106–111.
[18] B.H. Hameed, D.K. Mahmoud, A.L. Ahmad, Equilibrium modeling and kinetic studies on the adsorption of basic dye by a low-cost adsorbent: coconut (*Cocos nucifera*) bunch waste, J. Hazard. Mater., 158 (2008) 65–72.
[19] B.B. Mamba, N.P. Dlamin, A.F. Mulaba–Bafubiandi, Biosorptive removal of copper and cobalt from aqueous solutions: *Shewanella* spp. put to the test, Phys. Chem. Earth., 34 (2009) 841–849.
[20] J.W. Weber, P.M. McGinley, L.E. Katz, Sorption in subsurface systems: concept, models and effects on contaminant fate and transport, Water Res., 25 (1991) 499–528.
[21] Z.P. Gao, Z.F. Yu, T.L. Yue, S.Y. Quek, Adsorption isotherm, thermodynamics and kinetics studies of polyphenols separation from kiwifruit juice using adsorbent resin, J. Food Eng., 116 (2013) 195–201.
[22] N. Gandhi, D. Sirisha, K.B. Chandra Sekhar, Adsorption of fluoride (F^-) from aqueous solution by using pineapple (*Ananas comosus*) peel and orange (*Citrus sinensis*) peel powders, Int. J. Environ. Biorem. Biodegrad., 4 (2016) 55–67.
[23] M.I. Tempkin, V. Pyzhev, Kinetics of ammonia synthesis on promoted iron catalyst, Acta Phy. Chem., 12 (1940) 327–356.
[24] Y.S. HO, Citation review of Lagergren kinetic rate equation on adsorption reactions, Scientometrics, 59 (2004) 171–177.
[25] M. Asgher, H.N. Bhatti, Mechanistic and kinetic evaluation of biosorption of reactive azo dyes by free, immobilized and chemically treated *Citrus sinensis* waste biomass, Ecol. Eng., 36 (2010) 1660–1665.
[26] Y.S. Ho, Review of second-order models for adsorption systems, J. Hazard. Mater., 136 (2006) 6681–689.
[27] Y.S. Ho, G. McKay, A comparison of chemisorption kinetic models applied to pollutant removal on various sorbents, Process Saf. Environ. Prot., 76 (1998) 332–340.
[28] M.H. Kalavathy, T. Karthikeyan, S. Rajgopal, L.R. Miranda, Kinetic and isotherm studies of Cu(II) adsorption onto H_3PO_4 activated rubber wood sawdust, J. Colloid Interface Sci, 292 (2005) 354–362.
[29] S. Liang, X. Guo, N. Feng, Q. Tian, Isotherms, kinetics and thermodynamic studies of adsorption of Cu^{2+} from aqueous solutions by Mg^{2+}/K^+ type orange peel adsorbents, J. Hazard. Mater., 174 (2010) 756–762.
[30] F.C. Wu, R.L. Tseng, R.S. Juang, Characteristics of Elovich equation used for the analysis of adsorption kinetics in dye-chitosan systems, Chem. Eng. J., 150 (2009) 366–373.
[31] Y. Chen, W. Zhang, T. Zhao, F. Li, M. Zhang, J. Li, L. Yang, Adsorption properties of macroporous adsorbent resins for separation of anthocyanins from mulberry, Food Chem., 194 (2016) 712–722.
[32] J. Lee, R.W. Durst, R.E. Wrolstad, Determination of total monomeric anthocyanin pigment content of fruit juices, beverages, natural colorants, and wines by the pH differential method: collaborative study, J. AOAC Int., 88 (2005) 1269−1278.
[33] M. Turturică, A.M. Oancea, G. Râpeanu, G. Bahrim, Anthocyanins: naturally occurring fruit pigments with functional properties, Ann Univ Dunarea de Jos Galati. Fascicle VI, Food Technol., 39 (2015) 9–24.
[34] C. Beye, L.S. Tounkara, J. Destain, S. Zgoulli, A.S. Ndoye, P. Thonart, Study of the sorption behavior of *Hibiscus sabdariffa* anthocyanins on a macroporous resin, J. Food Process Eng., 36 (2013) 579–590.